

Predicting age and maturity of endangered Spiny butterfly ray, *Gymnura altavela* (Linnaeus 1758) using artificial neural network (multilayer perceptron)

Dr. Nader Iskandar Hamwi

Professor, Laboratory of Ichthyology, Agriculture Faculty, University of Tishreen,
Latakia, Syria.

Nader.hamwi@tishreen.edu.sy

Abstract

The data were derived from several sources, including 338 records of maturity, age, and disc width of the Spiny butterfly ray (*Gymnura altavela*). An artificial neural network (Multilayer Perceptron) model (1, 10, 2) was used to predict the maturity and age of the Spiny butterfly ray, which is a high-accurate model with excellent efficiency. This network shortens the time, effort and cost compared to traditional methods or a convolutional neural network (CNN) in age prediction. Therefore, we can predict the maturity and age of individuals without killing or harming them, just by getting simple data (disc width) and enter it into the updated model from the network. This network allows us to obtain valuable data for use in studying stock indicators of endangered Spiny butterfly ray without compromising their factual stock.

2022/06/02: Received

2022/08/04 Accepted:



Copyright:Damascus
University- Syria, The
authors retain the
copyright under a CC
BY- NC-SA

Key words: Age, Artificial Neural Network, *Gymnura altavela*, Maturity, Predicting.

التنبؤ بعمر ونضج الشفنين الفراشي الشوكي (*Gymnura altavela* Linnaeus 1758) المهده بالانقراض باستخدام الشبكة العصبية الاصطناعية (Multilayer Perceptron)

ا. د. نادر اسكندر حموي

مخبر الأسماك - كلية الهندسة الزراعية - جامعة تشرين - اللاذقية

Nader.hamwi@tishreen.edu.sy

المخلص

تم الحصول على البيانات من عدة مصادر، وقد تضمنت 338 سجلاً للنضج، والعمر، وعرض القرص disc width للشفنين الفراشي الشوكي (*Gymnura altavela*). واستخدم نموذج الشبكة العصبية الاصطناعية (Multilayer Perceptron) (1، 10، 2) للتنبؤ بنضج وعمر الشفنين الفراشي الشوكي، وهو نموذج عالي الدقة ذو كفاءة ممتازة، إذ تعمل هذه الشبكة على تقصير الوقت والجهد والتكلفة مقارنة بالطرق التقليدية أو الشبكة العصبية التلافيفية (CNN) في التنبؤ بالعمر. ولذلك، يمكننا التنبؤ بنضج وعمر الأفراد دون قتلهم أو إيدائهم عن طريق الحصول فقط على بيانات بسيطة (عرض القرص) وإدخالها في النموذج المحدث من الشبكة. وبالتالي نتيج لنا هذه الشبكة الحصول على بيانات قيمة لاستخدامها في دراسة مؤشرات المخزون للشفنين الفراشي الشوكي المهده بالانقراض دون المساس بمخزونه الحقيقي.

تاريخ الإيداع: 2022/07/04
تاريخ الموافقة: 2022/10/02



حقوق النشر: جامعة دمشق -
سورية، يحتفظ المؤلفون بحقوق

النشر بموجب الترخيص

CC BY-NC-SA 04

الكلمات المفتاحية: التنبؤ، العمر، النضج، الشبكة العصبية الاصطناعية، *Gymnura altavela*.

Introduction:

The traditional methods of determining age and maturity depend on killing and dissecting fish and extracting the appropriate structures for this purpose (scales, otolith, vertebrae, fin rays, gonads) after a manual preparation process (preserving, cutting, sanding, using chemicals, fixing), to be ready by researchers specialized in this field. This process is not easy, is expensive, requires significant time and effort, and can be subject to variations such as the differences in age estimation between researchers. Recently, a new method for estimating the age of fish has emerged, by relying on images of ear stones or vertebrae (such as CT scanning technologies for imaging otolith annular structure using the MARS Bioimaging Ltd X-ray scanning machine) and machine learning models or deep learning using a pre-trained convolutional neural network designed for object recognition, to estimate the age of fish from otolith images.

An application of artificial neural networks (ANNs) is an alternative modelling strategy for traditional methods of time series and data analysis. ANNs are computational algorithms that can fix composite problems that simplify biological brain operations (Lee *et al.*, 2019; Iliev, 2021). Perceptron neural networks include nodes or artificial neurons, which are data processing units arranged in layers and interrelated by synaptic weights (links). Neurons can filter and transfer data in a controlled manner to construct a predictive model that categorizes data saved in memory (Nemati *et al.*, 2015). The most important reason behind the widespread use of the artificial neural network is that it offers an efficient alternative to solving complex problems with classical statistical techniques and performs well in function approximation and pattern recognition (Lek and Guegan, 1999; Manoj *et al.*, 2014).

In the last few years, data-based techniques such as ANNs, fuzzy logic, genetic programming and support vector machines, have been widely used in the modelling of many composite problems (Suryanarayana *et al.*, 2008; Cabreira *et al.*, 2009; Yilmaz and Kaynar, 2011; Moen *et al.*, 2018; Hamwi and Ali-Basha, 2019; Moore *et al.*, 2019; Ordoñez *et al.*, 2020; Sangün *et al.*, 2020; Politikos *et al.*, 2021; Vabø *et al.*, 2021). Scientific references have pointed out that neural networks outperform all other methods in the extent of forecasting accuracy.

The Spiny butterfly ray has most recently been assessed for The IUCN Red List of Threatened Species in 2019. The Spiny butterfly ray is listed as Endangered under criteria A2d. They are slow-reproducing. The meat of this species is highly regarded and it is caught for human consumption (Dulvy *et al.*, 2021). Spiny butterfly rays are harmless to humans, though if stepped on its tail spine can cause a painful wound. It is listed as a game fish in some regions (Conrath and Scarbrough 2009). This study aimed to predict the age and maturity of endangered Spiny butterfly ray using an artificial neural network (Multilayer Perceptron) through a backpropagation algorithm as an effective proposed model compared to traditional methods that require great effort and may lead to human errors in estimation or calculations. This allows scientific experts interested in this field to determine the maturity and age of individuals simply and reliably and understand the true state of their growth within their current environment without causing any suffering to it, thus the possibility of guiding fishermen to avoid fishing its adult and mature individuals and continuing to preserve it.

Materials and methods:

The dataset used here included 338 records of maturity, age and disc width. The data were derived from several sources (Capapé, 1985; Gallart, 1998; Rizzo *et al.*, 1993; Ferreira *et al.*, 2008; Bradai *et al.*, 2012; Güven *et al.*, 2012; Pereira *et al.*, 2012; Alkusaairy, 2013; Froese and Pauly, 2022).

The spiny butterfly ray (*Gymnura altavela*) is a species of butterfly ray, family Gymnuridae, native to the shallow coastal waters of the Atlantic Ocean. A large ray that can measure over 2 m (6 ft 7 in) across, it may be distinguished from the sympatric smooth butterfly ray (*G. micrura*) by the spine at the base of its tail and by a small tentacular structure on the margin of each spiracle. This species has a patchy and discontinuous distribution in Atlantic tropical and warm-temperate waters. In the western Atlantic; it is rare in the Gulf of Mexico and common in the mouths of tidal creeks along the Virginia coast. In the eastern Atlantic, it is found from Portugal to Ambriz, Angola, including the Mediterranean Sea, the Black Sea, and the Madeira and Canary Islands. It is found in shallow brackish

and coastal waters over soft sandy or muddy substrates, at a depth of 5–100 m (16–328 ft). This ray is uncommon overall but can be locally abundant in suitable habitat. Individuals may segregate by sex, with females usually staying in deeper water but moving inshore to breed (Wikipedia, 2022) (Figure 1, a).

The spiny butterfly ray has a very broad, lozenge-shaped pectoral fin disk much wider than it is long, with concave front margins and abruptly rounded corners. The snout is short and blunt. The teeth have high, conical cusps, numbering 98–138 rows in the upper jaw and 78–110 rows in the lower jaw. In both jaws there are 10–12 functional tooth rows with each dental band occupying 70% the width of the jaw. There is a tentacle-like structure on the inner posterior margin of each spiracle. The tail is short and slender, measuring a quarter the disk width, with upper and lower fin folds. There are one or more serrated spines at the base of the tail. The skin is naked in juveniles and subadults, while adults develop a patch of denticles on the center of the disk. The coloration is dark brown above, sometimes with small lighter or darker spots and blotches in a marbled pattern, and white below. Juveniles have pale crossbars on the tail. The maximum reported size is 2.2 m (7 ft 3 in) disk width in the northwest Atlantic, though there are unsubstantiated reports of rays over 4 m (13 ft) off West Africa. The maximum published weight is 60 kg (130 lb) (Figure 1, b). Spiny butterfly rays are ovoviviparous and give birth to live young. They have an annual reproductive cycle with a gestation period of 4 to 9 months. The embryos initially subsist on a yolk sac; later in development long villi develop from the uterine wall into the embryos' spiracles, which direct uterine milk into the oral cavity. Litter size is up to 8, depending on geographical location: 4 per litter in the Gulf of Mexico, 1–6 in the Mediterranean, up to 5 off Brazil, and up to 8 in the northwest Atlantic. Females have one functional ovary (the left) and two functional uteruses, with the embryos evenly distributed in each one. The newborns measure 38–44 cm (15–17 in) across; their size is inversely related to the number of young in each uterus. In the eastern Atlantic, males mature at around 78 cm (31 in) across and females at 108 cm (43 in). In the western Atlantic, males mature at around 102 cm (40 in) across and females at 155 cm (61 in). Females mature later than males and reach a larger size (Wikipedia, 2022).



**Figure 1. a, Range of the spiny butterfly ray (*Gymnura altavela*).
b, *Gymnura altavela* (Adib and Alkusairy, 2022).**

To set up the neural network model and test its accuracy was used the Multi-layer Perceptron (MLP) Module of MATLAB R2022a software, was trained with a back-propagation learning algorithm that uses gradient descent to update the weights for decreasing the error function. The training dataset is utilized to find the weights and set up the model. The testing data is utilized to find errors and avert overtraining during the training pattern (training algorithm: Levenberg Marquardt). The validation data is utilized to validate the model. Before training, all covariates were normalized utilizing the formula $(x - \min) / (\max - \min)$, which returns values between 0 and 1, and data only from the training set.

Input vector (P): Disc width (arranged from 17.70 to 215 cm) (Wigley *et al.*, 2003; Baçusta *et al.*, 2012; Ozbek *et al.*, 2016; Parsons *et al.*, 2018; Yeldan, 2018).

Target vectors (Y):

Y1: Age (arranged from 0 to 18 years) (Parsons *et al.*, 2018).

Y2: Maturity (Immature = 0; Mature =1): Males and females mature at 38 cm in disc width, respectively (Alkusaury, 2013) (Table 1).

Table 1. Summary of statistical parameters of input and output variables (n = 338)

Variable	Unit	Min	Max	Median	Mean	SD
Input						
Disc width	cm	17.70	215	21.04	31.12	35.64
Output						
Maturity	[0,1]	0	1	0	0.41	0.49
Age	year	0	18	1	4.53	5.13

SD standard deviation

They will be randomly divided into three sets so that 70% are used for training, 15% are used to validate that the network is generalizing and to stop training before overfitting. The last 15% are used as a completely independent test of network generalization. At the hidden layer, each neuron calculates, $n1$, a weighted sum (IW_{ji}) of input signals, P_i , for $i = 1, 2, \dots, n$, and then applies a nonlinear activation function to create an output signal, $a1$, and at the output layer, each neuron calculates, $n2$, a weighted sum (LW_{ji}) of an output signal, $a1$, and then applies a linear activation function to create an output signal, $a2$. The model of a neuron is shown in figure (2).

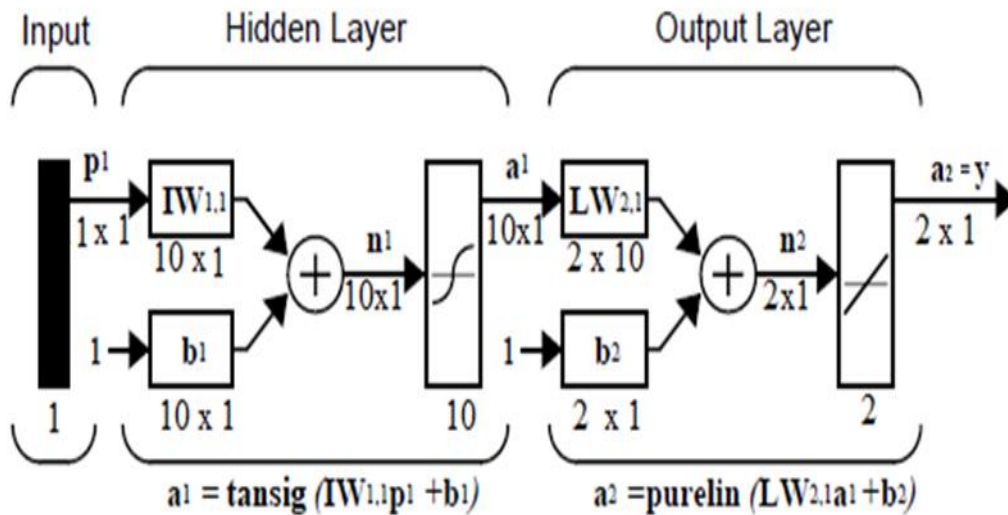


Figure 2. Neural network: multilayer perceptron (MLP) (by author).

A neuron j is described mathematically by the following equations:

$$n1 = \sum_{i=1}^n IW_{1,i} \cdot P_i$$

And

$$a1 = \text{tansig}(IW_{1,i} \cdot P_i + b_{1,i})$$

Then

$$n2 = \sum_{i=1}^n LW_{2,i} \cdot a1,i$$

And

$$a2 = \text{purelin}(LW_{2,i} \cdot a1,i + b_{2,i}) = Y$$

Where b is the bias term of the j th neuron (Haykin and Network, 2004; Melesse and Hanley, 2005). The tangent sigmoid nonlinear function (Bilgili *et al.*, 2007) is used for this purpose, expressed as:

$$\text{tansig} = \frac{2}{1 + e^{-2x}} - 1$$

The default performance function for feedforward networks is MSE — the average squared error among the network outputs a and the target outputs Y :

$$MES = \frac{1}{n} \sum_{i=1}^n (Y_{\text{true}} - Y_{\text{pred}})^2$$

Results and discussion:

The ANN (1, 10, 2) was selected as the ideal ANN model by MATLAB R2022a software (Figure 3). The network was trained to 107 epochs utilization of the Levenberg–Marquardt learning algorithm with a mu of 1.00E-6 (Figure 4).

The optimal neurons number in the hidden layer was determined by utilising a trial-and-error process by variable hidden neurons number from 1 to 10. The hidden neurons number supplying the optimal building was fixed as 10. This training stopped when the validation error increased, which occurred after 107 iterations. Training produces a plot of the training errors (MSE = 0.0467765 and R = 0.998619), validation errors (MSE = 0.022662 and R = 0.998813) and test errors (MSE = 0.0245610 and R = 0.999200), as shown in the following figure (5).

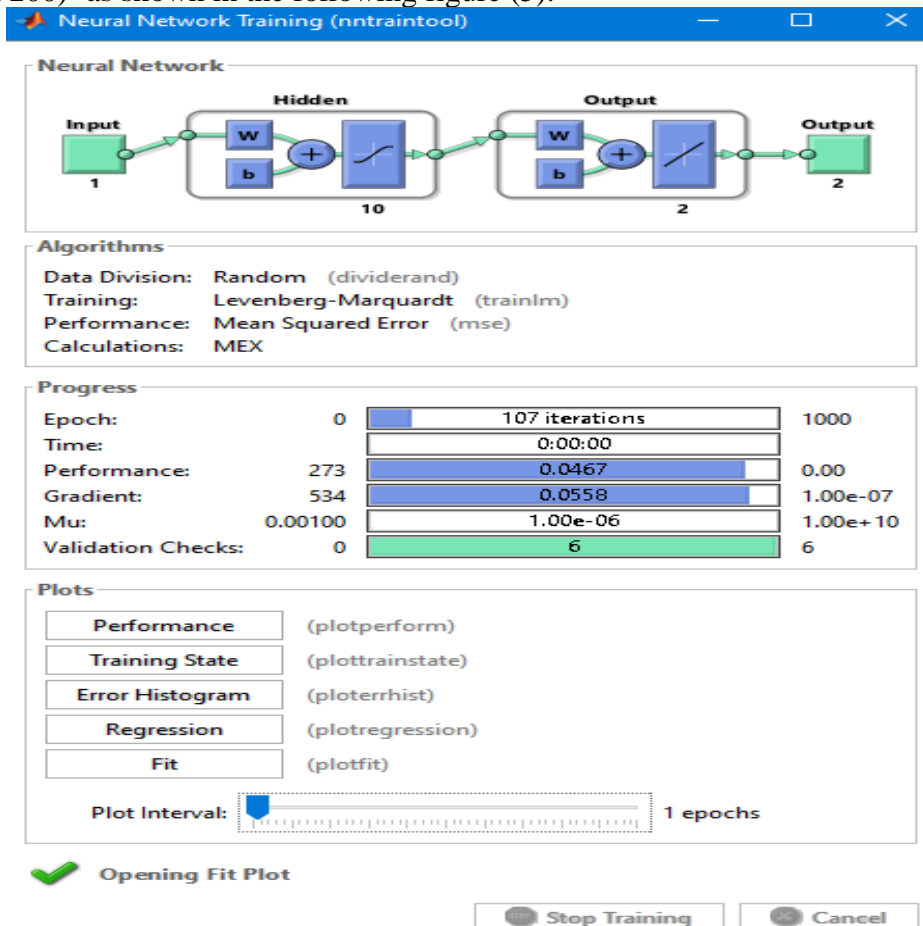


Figure 3. The ANN model (1, 10, 2) by MATLAB R2022a software.

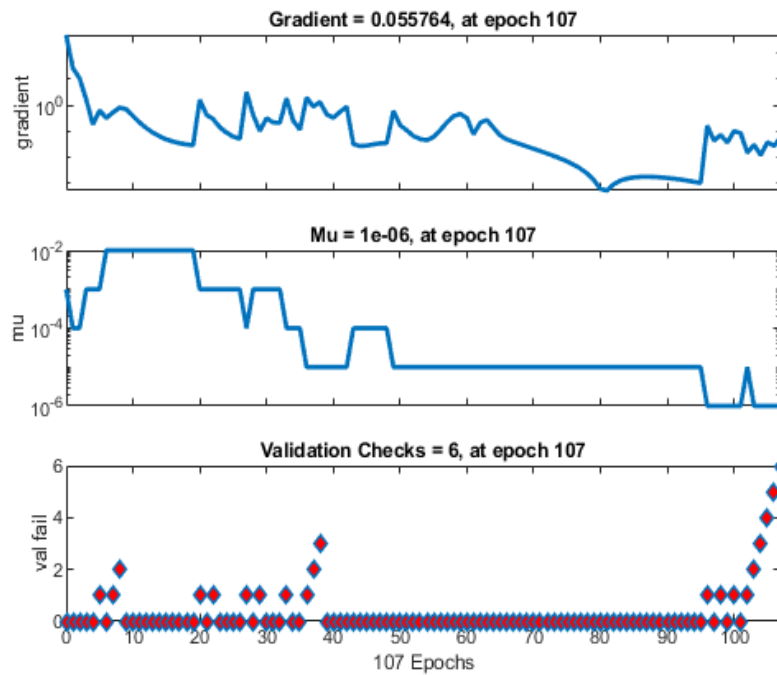


Figure 4. Plot training state to 107 epochs.

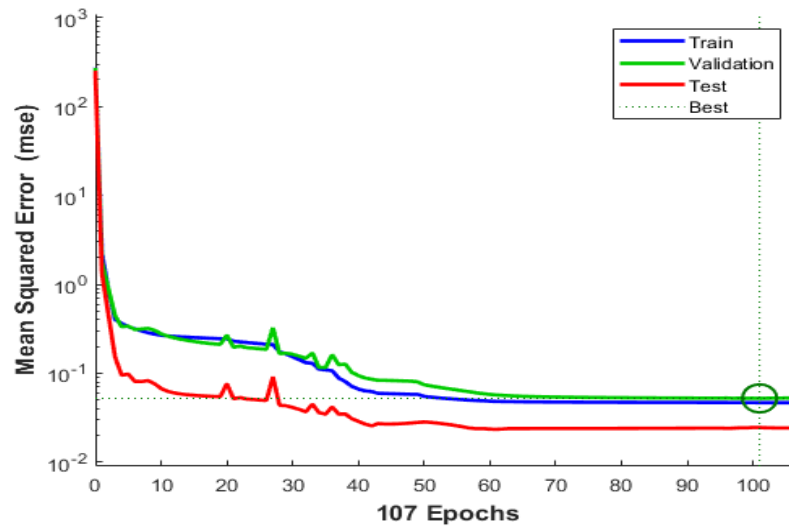


Figure 5. Best validation performance is 0.052266 at epoch 101.

In this study, the result was reasonable because the final mean square error (MSE) was small (Figure 6), the test set error and the validation set error have similar characteristics, and no significant overfitting has occurred by epoch 101 (with the most validation performance happening) (Figure 5).

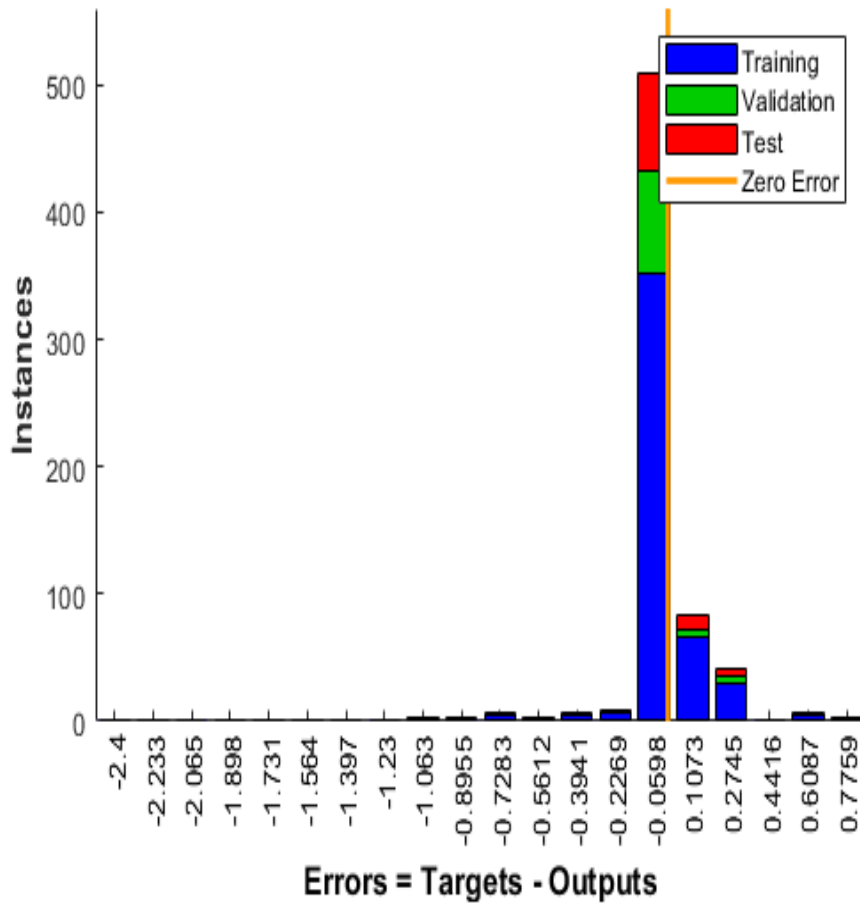


Figure 6. Error histogram with 20 Bins for the ANN model.

The output tracks the responses considerably for training, validation and testing sets, and the R-value is 0.99873 (a close relationship) for the total dataset (Figure 7). The synaptic weights and biases of this network, which were computed from the training dataset only, were represented as evident from table (2). The plot fit (net, inputs, targets) plots the output function of a network across the range of the inputs and also plots target targets and output data points associated with values in inputs. The error bars show the difference between outputs and targets (Figure 8).

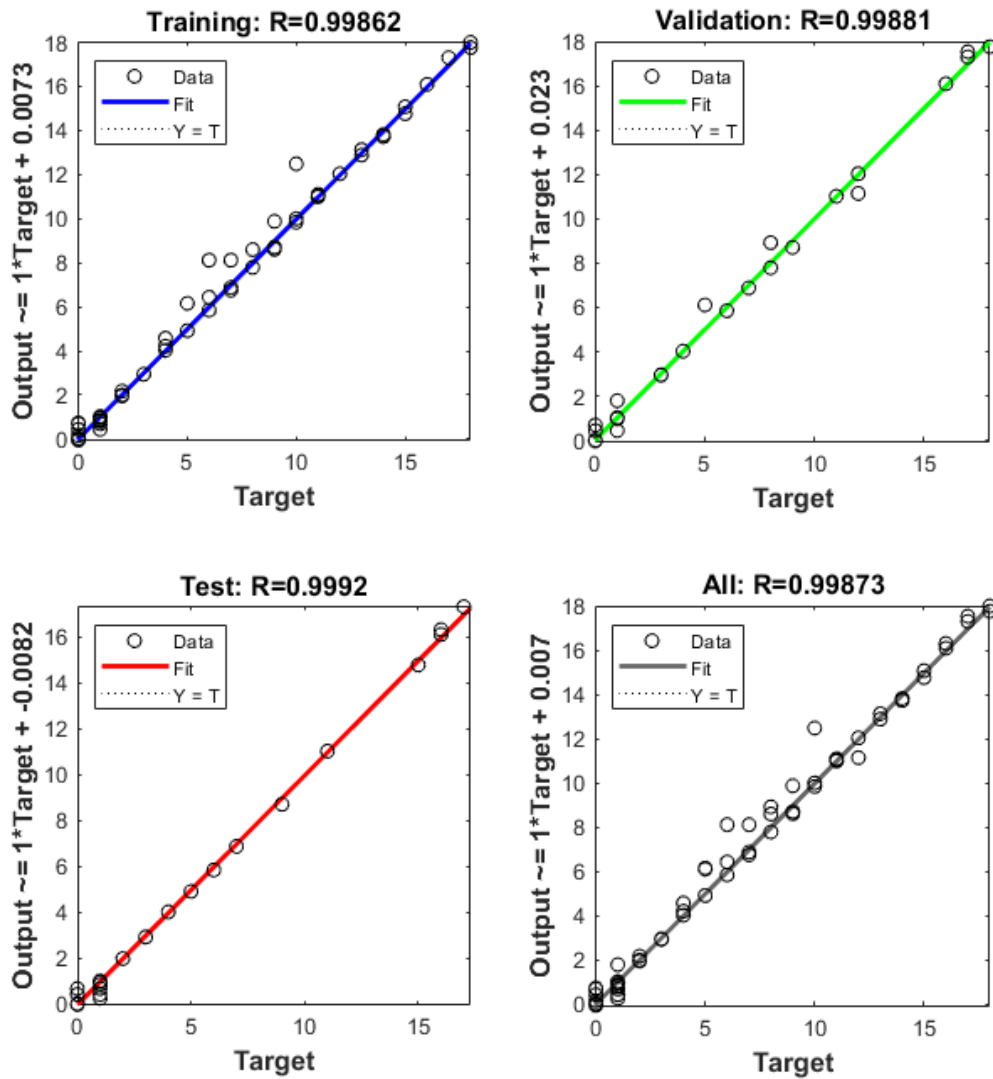


Figure 7. Neural network training regression (plot regression) epoch 107, validation stop.

Table 2. Weights and bias of training dataset by ANN.

Weights W1 =										Bias b1 =	
											9.5222
											-9.2425
											15.1532
											0.6351
											-12.7237
											0.6576
											-0.9882
											13.9905
											-10.5809
											11.2100
Weights W2 =											
-0.5170	0.1314	4.7575	2.9579	4.2904	-3.5521	-0.3903	0.8789	1.2136	0.3198		
-0.0049	-0.0458	-0.1083	1.2160	-0.1816	-1.0505	-1.6971	-3.0660	-5.0034	-2.2717		
Bias b2 =											
0.1143											
-0.0749											

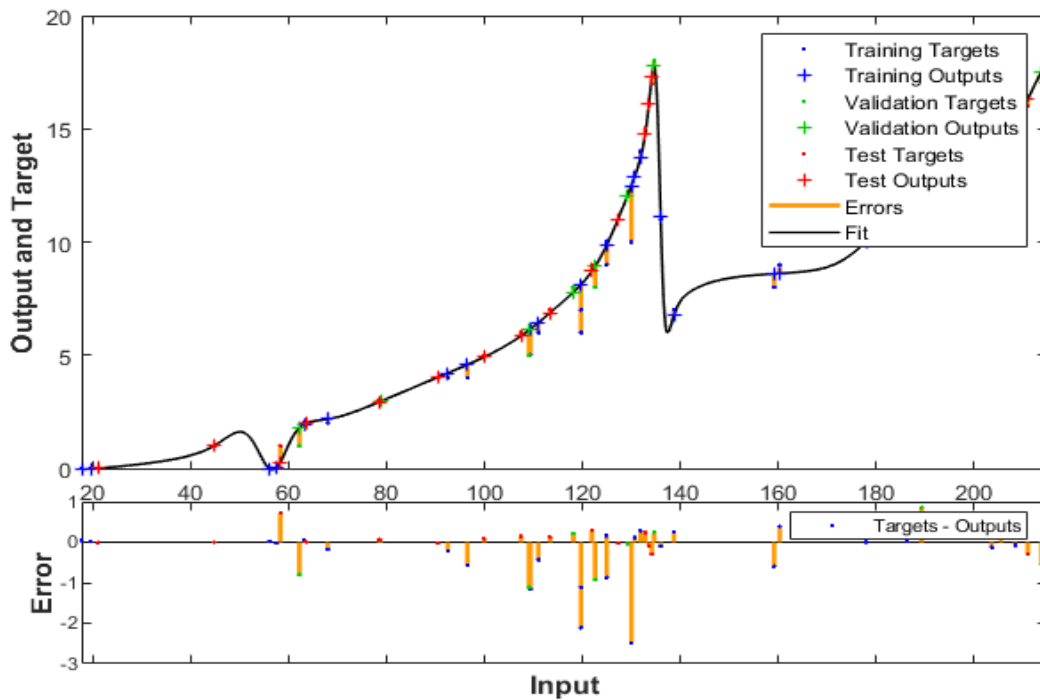


Figure 8. Function fit for output element..

To clarify the work of the ANN and its accuracy in its prediction of the maturity and age of the Spiny butterfly ray, it was tested through 10 new and random samples consecutively of the disc widths of the Spiny butterfly ray (Table 3), where high accuracy was observed in estimating the maturity and age, during the matching of the predicted values with the real values. test errors (Maturity: MSE= 4.1E-07 and R = 0.96; Age: MSE= 3.87E-0.6 and R = 0.9998).

Table 3. Testing random samples (Disc width, cm) on the ANN model accuracy for estimation of maturity and age of the Spiny butterfly ray.

Disc width	Human (reading)		ANN (Testing)	
	Maturity	Age	Maturity	Age
21.04	0	0	0.00202	0.0062173
44.77	0	1	0.00028	1.0008
63.61	0	2	0.00850	1.9984
90.49	1	4	0.69374	4.0257
118.16	1	8	1.02860	7.7849
124.92	1	10	0.99050	9.8379
127.3	1	11	0.98682	11.0151
129.19	1	12	0.99008	12.0346
130.69	1	13	0.99548	12.8829
134.66	1	18	0.99430	17.7581

Work on neural networks in the 1980s and 1990s was limited by low computational power, lack of large data sets for training, and limitations in machine learning algorithms (Malde *et al.*, 2019). In recent years, increasing parallel processing capabilities (for example, using GPUs), declining computing hardware costs, distributed computing, and advances in machine learning algorithms have led to the creation of much larger and deeper neural networks than ever before.

Most of the current recent research based on machine learning or deep learning (the convolutional neural network) to determine the age of bony fish is focused on processing images of ear stones or scales and their approach to those taken previously. While there are no studies on the use of deep learning technology in automating the lifespan of cartilaginous fish. Rather, evaluation is limited to

the use of micro-computed tomography as a valid and reproducible alternative approach to determining age in the Spinner shark, *Carcharhinus brevipinna*. High-resolution X-rays have also been used by Parsons *et al.* (2018) to provide images of vertebrae for age estimation in rays of the Spiny butterfly ray, *Gymnura Altavela*, from the North Atlantic. Although the numbers of episodes from the reconstructed images were not tested against those of severed vertebrae, the CT images revealed interpretable growth bands that were read with high accuracy between and within readers. Francis *et al.* (2018a, 2018b) experimented with the use of vertebral computed tomography scanning technology to estimate age in common (*Tetronarce nobiliana*), blind electromyography (*Typhlonarke aysoni*), shark (*Cephaloscyllium isabellum*) and four species of the deep-water shark, which are the seal shark (*Dalatias licha*), the Austin seal shark (*Centroscymnus owstonii*), the long-nosed velvet sea dog (*Centroselachus crepidater*), and the Plunket shark (*Scymnodon plunketi*). Politikos *et al.* (2021) found that a network without multitasking learning correctly predicted the age of fish by 64.4%, and achieved high performance for younger age groups (0 and 1, F1 score > 0.8) and moderate performance for the older age groups (2 to 5+, grade F1 score: 0.50 x 0.54). The network with multitasking learning increased the correctness of age prediction up to 69.2% and was shown to be effective in making use of its predictive performance for older age groups (2 to 5+, F1: score 0.57-0.64). Moen *et al.* (2018) adapted a pre-trained convolutional neural network designed for object recognition, to estimate the age of fish from otolith images of Greenland halibut, and showed that the model works well and that its precision is comparable to documented precision obtained by human experts. Moore *et al.* (2019) found after training of convolutional neural network (CNN), the model gave the same age as the human reader for 47% of Snapper (*Pagrus auratus*) in a test dataset, with a further 35% of ages estimated within 1 year of the human reader estimate of age. For Hoki (*Macruronus novaezelandiae*), the model gave the same age as the human reader for 41% of individuals. Vabø *et al.* (2021) applied Convolutional Neural Networks (CNN) with transfer learning on images of Atlantic salmon scales for four different prediction tasks. They obtained high prediction accuracy for fish origin (96.70%), spawning history (96.40%), and sea age (86.99%), but lower accuracy for river age (63.20%).

Despite these attempts to use the convolutional neural network to predict an age by processing images of otolith and sometimes scales, its performance is still weak. Not to mention the great difficulty in the additional procedures and the expensive and complex equipment for preparing the sections of these otoliths and thus obtaining cross-sectional images of them in order to identify them and compare them with the original results documented by the researchers previously. All of this increases the complexity and difficulty of the matter and does not provide a simple and easy solution that dispenses with the time and great effort of preparation as well as costs.

The proposed artificial neural network (Multilayer Perceptron) model (1, 10, 2) is a high-accurate model with excellent effectiveness in predicting the maturity and age of the Spiny butterfly ray. The current ANN shorten the time, effort and cost against the traditional methods or a convolutional neural network (CNN). We can predict the maturity and age of individuals without killing or harming them, just by having simple data (disc width). Thus, this network allows us to obtain valuable data for use in studying stock indicators of endangered Spiny butterfly ray without compromising their factual stock.

In future, the current network can add new data from researchers interested in this field and increase its training and accuracy capacity in giving the required results.

References:

1. Alkusaury, H. H. (2013). The life cycle of cartilaginous species: *Gymnura altavela* (Linnaeus 1758) (Gymnuridae) in Syrian marine water. Iraqi Journal of Aquaculture, 10 (2).
2. Başusta, A., Başusta, N., Sulikowski, J.A., Driggers, W.B., Demirhan, S.A., and Cicek, E. (2012). Length–weight relationships for nine species of batoids from the Iskenderun Bay, Turkey. Journal of Applied Ichthyology 28(5): 850-851.
3. Bilgili, M., Sahin, B., and Yasar, A. (2007). Application of artificial neural networks for the wind speed prediction of target station using reference stations data. Renew Energy, 32, 2350–2360.
4. Bradai, M.N., Saidi, B. and Enajjar, S. (2012). Elasmobranchs of the Mediterranean and Black sea: status, ecology and biology. Bibliographic analysis. Studies and Reviews. General Fisheries Commission for the Mediterranean. No. 91. Rome, FAO. 103 pp.
5. Cabreira, A. G., Tripode, M., and Madirolas, A. (2009). Artificial neural networks for fish-species identification. ICES Journal of Marine Science, 66 (6), 1119-1129.
6. Capapé, C. (1985). Nouvelle description de *Centrophorus granulosus* (Schneider, 1801) (Pisces, Squalidae). Données sur la biologie de la reproduction et le régime alimentaire des spécimens des côtes tunisiennes. Bull. Inst. Natn. Scient. Tech. Océanogr. Pêche Salambô 12: 97–141.
7. Conrath, C. and Scarbrough, R. (2009). Biological Profiles: Spiny Butterfly Ray. Florida Museum of Natural History Ichthyology Department. Retrieved on March 4.
8. Dulvy, N.K., Charvet, P., Carlson, J., Badji, L., Blanco-Parra, MP, Chartrain, E., De Bruyne, G., Derrick, D., Dia, M., Doherty, P., Dossa, J., Ducrocq, M., Leurs, G.H.L., Notarbartolo di Sciara, G., Pérez Jiménez, J.C., Pires, J.D., Seidu, I., Serena, F., Soares, A., Tamo, A., Vacchi, M., Walls, R.H.L. and Williams, A.B. (2021). *Gymnura altavela*. The IUCN Red List of Threatened Species 2021: e.T63153A3123409. <https://dx.doi.org/10.2305/IUCN.UK.2021-1.RLTS.T63153A3123409.en>. Accessed on 19 September 2022.
9. Ferreira, S., Sousa, R., Delgado, J., Carvalho, D. and Chada, T. (2008). Weight-length relationships for demersal fish species caught off the Madeira archipelago (eastern-central Atlantic). J. Appl. Ichthyol. 24:93-95. <http://dx.doi.org/10.1111/j.1439-0426.2007.01027.x>
10. Francis, M.P., Ó Maolagáin, C. and Lyon, W.S. (2018a). Growth and reproduction of carpet shark, common electric ray and blind electric ray in New Zealand waters. New Zealand Aquatic Environment and Biodiversity Report No. 195. 39 p.
11. Francis, M.P., Jones, E.G., Ó Maolagáin C. and Lyon, W.S. (2018b). Growth and reproduction of four deepwater sharks in New Zealand waters. New Zealand Aquatic Environment and Biodiversity Report No. 196. 58 p.
12. Froese, R. and Pauly D. (2022). FishBase. World Wide Web electronic publication. www.fishbase.org, version (06/2022).
13. Gallart, J. (1998). Contribución al conocimiento de la taxonomía y la biología del tiburón batial *Centrophorus granulosus* (Bloch & Schneider, 1801) (Elasmobranchii, Squalidae) en el Mar Balear (Mediterráneo occidental). Ph.D Thesis, Universitat de Valencia, Valencia: 291p.
14. Güven, O., Kebapçioğlu, T. and Deval, M.C. (2012). Length-weight relationships of sharks in Antalya Bay, eastern Mediterranean. J. Appl. Ichthyol. 28:278-279. <http://dx.doi.org/10.1111/j.1439-0426.2011.01823.x>
15. Hamwi, N. and Ali Basha, N. (2019). Estimation of the vulnerability of some Sparidae species to fishing in the Eastern Mediterranean Sea (Syrian coast) by fuzzy logic method. Journal of Al-Baath University, vol. 41, No. 10, 129-160.
16. Haykin, S. and Network, N. (2004). A comprehensive foundation. Neural networks, 2 (2004), 41.
17. Iliev, A. (2021). Modern Challenges in Machine Learning and Artificial Intelligence. Digital Presentation and Preservation of Cultural and Scientific Heritage, (XI), 33-40.

18. Lee, J., Xiao, L., Schoenholz, S., Bahri, Y., Novak, R., Sohl-Dickstein, J. and Pennington, J. (2019). Wide neural networks of any depth evolve as linear models under gradient descent. *Advances in neural information processing systems*, 32, 8572-8583.
19. Lek, S. and Guégan, J. F. (1999). Artificial neural networks as a tool in ecological modelling, an introduction. *Ecological modelling*, 120 (2-3), 65-73.
20. Malde, K., Handegard, N.O., Eikvil, L. and Salberg, A.B. (2019). Machine intelligence and the data-driven future of marine science. *ICES Journal of Marine Science*, fsz057, <https://doi:10.1093/icesjms/fsz057>.
21. Manoj, M., Gandhi, R.S., Raja, T.V., Ruhil, A.P., Singh, A. and Gupta, A.K. (2014). Comparison of artificial neural network and multiple linear regression for prediction of first lactation milk yield using early body weights in Sahiwal cattle. *Indian Journal of Animal Sciences*, 84427, (4)–430.
22. Melesse, A. M. and Hanley, R. S. (2005). Artificial neural network application for multiecosystem carbon flux simulation. *Ecol Model*, 189, 305–314.
23. Moen, E., Handegard, N. O., Allken, V., Albert, O. T., Harbitz, A. and Malde, K. (2018). Automatic interpretation of otoliths using deep learning. *PLoS One*, 13(12), e0204713. <https://doi.org/10.1371/journal.pone.0204713>.
24. Moore, B. R., Maclaren, J., Peat, C., Anjomrouz, M., Horn, P. L. and Hoyle, S. (2019). Feasibility of automating otolith ageing using CT scanning and machine learning. *New Zealand Fisheries Assessment Report*, 58, 23.
25. Nemati, S., Fazelifard, M. H., Terzi, Ö. and Ghorbani, M. A. (2015). Estimation of dissolved oxygen using data-driven techniques in the Tai Po River, Hong Kong. *Environmental earth sciences*, 74 (5), 4065-4073.
26. Ordoñez A, Eikvil L, Salberg A-B, Harbitz A, Murray S.M. and Kampffmeyer MC (2020). Explaining decisions of deep neural networks used for fish age prediction. *PLoS ONE*, 15 (6): e0235013. <https://doi.org/10.1371/journal.pone.0235013>.
27. Ozbek, E.O, Çardak, M. and Kebapçioğlu, T. (2016). Spatio-temporal patterns of abundance, biomass and length-weight relationships of *Gymnura altavela* (Linnaeus, 1758) (Pisces: Gymnuridae) in the Gulf of Antalya, Turkey (Levantine Sea). *J. Black Sea/Mediterranean Environment*, Vol. 22, No. 1: 16-34.
28. Parsons. K.T., Maisano.J., J. Gregg., C., Cotton C.F and Latour, R. J. (2018). Age and growth assessment of western North Atlantic spiny butterfly ray *Gymnura altavela* (L. 1758) using computed tomography of vertebral centra. *Environ Biol Fish* 101:137–151 <https://doi.org/10.1007/s10641-017-0687-x>.
29. Pereira, J.N., Simas, A., Rosa, A., Aranha, A., Lino, S., Constantino, E., Monteiro, V., Tariche, O. and Menezes, G. (2012). Weight-length relationships for 27 demersal fish species caught off the Cape Verde archipelago (eastern North Atlantic). *J. Appl. Ichthyol.* 28:156-159. <http://dx.doi.org/10.1111/j.1439-0426.2011.01915.x>
30. Politikos, D. V., Petasis, G., Chatzisprou, A., Mytilineou, C. and Anastasopoulou, A. (2021). Automating fish age estimation combining otolith images and deep learning: The role of multitask learning. *Fisheries Research*, 242, 106033.
31. Rizzo P., Gangitano S., Cannizzaro L., Levi D. and Mulone S. (1993). Determinazione dell'età e accrescimento in *Centrophorus granulosus* (Schneider, 1801). *Biologia Marina, Suppl. al Notiziario S.I.B.M.*(1), p389.
32. Saad, A., and Alkusaairy, H. H. (2022). Atlas (illustrated guide) of cartilaginous fishes (sharks, rays, and chimeras) in Syrian marine waters; How to identify and classify them, their biological properties, their range of distribution. Tishreen University and the Syrian Society for Aquatic Environment Protection (SSAEP), 95 p.

33. Sangün, L., Güney, O. I., Özalp, P. and Başusta, N. (2020). Estimation of body weight of *Sparus aurata* with artificial neural network (MLP) and M5P (nonlinear regression)–LR algorithms. *Iranian Journal of Fisheries Sciences*, 19 (2), 541-550. DOI: 10.22092/ijfs.2018.117010.
34. Suryanarayana, I., Braibanti, A., Rao, R. S., Ramam, V. A., Sudarsan, D. and Rao, G. N. (2008). Neural networks in fisheries research. *Fisheries Research*, 92 (2-3), 115-139.
35. Vabø, R., Moen, E., Smoliński, S., Husebø, Å., Handegard, N. O. and Malde, K. (2021). Automatic interpretation of salmon scales using deep learning. *Ecological Informatics*, 63, 101322.
36. Wigley, S. E., McBride, H. M. and McHugh, N. J. (2003). Length-weight relationships for 74 fish species collected during NEFSC research vessel bottom trawl surveys, 1992-99.
37. Wikipedia contributors. (2022, April 29). Spiny butterfly ray. In Wikipedia, The Free Encyclopedia. Retrieved 11:51, September 19, 2022, from https://en.wikipedia.org/w/index.php?title=Spiny_butterfly_ray&oldid=1085225502.
38. Yeldan, H. (2018). Estimating some population parameters and stock assesment of spiny butterfly ray, *Gymnura altavela* (Linnaeus, 1758) the Levant Basin coast (Northeastern Mediterranean). *Indian Journal of Animal Research*, 52(12), 1790-1796. DOI: 10.18805/ijar.B-917.
39. Yilmaz, I. and Kaynar, O. (2011). Multiple regression, ANN (RBF, MLP) and ANFIS models for prediction of swell potential of clayey soils. *Expert Syst Appl*, 38, 5958–5966.